Synthesis, X-ray Crystal Structures, and Gas Sorption Properties of Pillared Square Grid Nets Based on Paddle-Wheel Motifs: Implications for Hydrogen Storage in Porous Materials

ARTICLE *in* CHEMISTRY · JUNE 2005

Impact Factor: 5.73 · DOI: 10.1002/chem.200401201 · Source: PubMed

4 AUTHORS, INCLUDING:

Kimoon Kim
Pohang University of Science and Technology
298 PUBLICATIONS **19,385** CITATIONS

SEE PROFILE

VIP

Synthesis, X-ray Crystal Structures, and Gas Sorption Properties of Pillared Square Grid Nets Based on Paddle-Wheel Motifs: Implications for Hydrogen Storage in Porous Materials

Hyungphil Chun, Danil N. Dybtsev, Hyunuk Kim, and Kimoon Kim*[a]

Abstract: A systematic modulation of organic ligands connecting dinuclear paddle-wheel motifs leads to a series of isomorphous metal-organic porous materials that have a three-dimensional connectivity and interconnected pores. Aromatic dicarboxylates such as 1,4-benzenedicarboxylate (1,4-bdc), tetramethylterephthalate (tmbdc), 1,4-naphthalenedicarboxylate (1,4-ndc), tetrafluoroterephthalate (tfbdc), or 2,6-naphthalenedicarboxylate (2,6-ndc) are linear linkers that form two-dimensional layers, and diamine ligands, 4-diazabicyclo[2.2.2]octane (dabco) or 4,4′-dipyridyl (bpy), coordinate at both sides of Zn_2 paddle-wheel units to bridge the layers vertically. The resulting open frameworks $[Zn_2(1,4\text{-bdc})_2(dabco)]$ (**1**), $[Zn_2(1,4\text{-bdc})(tmbdc)(dabco)]$ (**2**), $[Zn_2(tmbdc)_2(dabco)]$ (**3**), $[Zn_2(1,4\text{-ndc})_2(dabco)]$ (**4**), $[Zn_2(tfbdc)_2(dabco)]$ (**5**), and $[Zn_2(tmbdc)_2(bpy)]$ (**8**) possess varying size of pores and free apertures originating from the side groups of the 1,4-bdc derivatives. $[Zn_2(1,4\text{-bdc})_2(bpy)]$ (**6**) and $[Zn_2(2,6\text{-ndc})_2(bpy)]$ (**7**) have two- and threefold interpenetrating structures, respectively. The non-interpenetrating frameworks (**1**–**5** and **8**) possess surface areas in the range of 1450–2090 m^2g^{-1} and hydrogen sorption capacities of 1.7–2.1 wt% at 78 K and 1 atm. A detailed analysis of the sorption data in conjunction with structural similarities and differences concludes that porous materials with straight channels and large openings do not perform better than those with wavy channels and small openings in terms of hydrogen storage through physisorption.

Keywords: coordination polymers · gas sorption · hydrogen · microporous materials · zinc

Introduction

One of the most important developments in chemical research in this decade will involve studies on coordination polymers with a crystal lattice. According to a survey reported in a recent review,[1a] more than one thousand reports are projected to appear on the topic within this year. Metal-organic open frameworks, coordination polymers with a void space accessible to various guest molecules, are gaining importance accordingly. Although it has been only a few years since the first reports of such materials with a permanent porosity,[2] many review articles have been dedicated to the structural and functional aspects of metal-organic open frameworks.[1] The strong interests in this field are partly due to intrinsic advantages over conventional porous materials, such as activated carbons and zeolites. They include facile syntheses based on the self-assembly of molecular components and the highly crystalline nature of products, which not only allows single-crystal X-ray diffraction analysis, but also guarantees the reproducibility and consistency of physical properties. Besides, the well-defined geometry of molecular components significantly improves the predictability of the crystalline phase of products. Of special interests among the advantageous properties pertinent to the present work is the ability to modify pore environments while maintaining the topology of the host framework.[3]

As the automobile and fuel cell industry looks for an efficient method to store and transport hydrogen,[4] metal-organic porous materials have been closely examined for their gas sorption properties. The results from recent papers on hydrogen sorption in metal-organic porous materials,[5] however, do not converge to a singular conclusion that might be

[a] Dr. H. Chun, Dr. D. N. Dybtsev,[+] H. Kim, Prof. Dr. K. Kim
National Creative Research Initiative Center for Smart Supramolecules, and Department of Chemistry, Division of Molecular and Life Sciences
Pohang University of Science and Technology
San 31 Hyojadong, Pohang 790–784 (Republic of Korea)
Fax: (+82) 54-279-8129
E-mail: kkim@postech.ac.kr

[+] Permanent address: Institute of Inorganic Chemistry 3, Lavrenteva St., Novosibirsk, 630090 (Russia)

Supporting information for this article is available on the WWW under http://www.chemeurj.org/ or from the author.

 DOI: 10.1002/chem.200401201

helpful in the future development of this area. For example, it is not clear whether a porous material with a higher surface area always uptakes more hydrogen than others, whether hydrogen adsorbs better on a certain surface than others, or whether it is possible to influence hydrogen sorption in porous materials with chemical functionalities.

This study is an effort to gain an insight into these questions, and here we present single-crystal X-ray structures and gas sorption properties of metal-organic frameworks that are systematically modulated from a prototype that we have reported recently.[5a] The original framework $[Zn_2(1,4\text{-bdc})_2(dabco)]$ (**1**) displays relatively high H_2 sorption capacity, namely 2.0 wt% at 78 K and 1 atm. Therefore, we set out to vary the ligands, 1,4-bdc (1,4-benzenedicarboxylate) and dabco (1,4-diazabicyclo[2.2.2]octane), without altering the overall connectivity of the nets and to monitor the differences in H_2 gas sorption behavior under the same conditions. The dicarboxylate and diamine ligands used to construct the sister nets are shown in Scheme 1. First, a dicarboxylate linker with aliphatic (tetramethylterephthalate, tmbdc), aromatic (1,4-naphthalenedicarboxylate, 1,4-ndc), or halogenic (tetrafluoroterephthalate, tfbdc) side groups on the phenyl ring was used instead of 1,4-bdc in **1**, which resulted in a series of isomorphous frameworks **2**–**5**. Then, the linker and diamine pillar in **1** were replaced with longer ones, such as, 2,6-naphthalenedicarboxylate (2,6-ndc) and 4,4′-dipyridyl (bpy), respectively, and frameworks **6**–**8** were obtained. Structural features arising from the substitutions and results of gas sorption experiments will be discussed in detail in order to draw a conclusion which may be useful in designing a new metal-organic porous material for gas-storage applications.

Results and Discussion

Synthesis and structural characterization: The so-called "pillaring" strategy[6] in designing metal-organic open frameworks involves using appropriate pillars to connect well-defined two-dimensional (2D) layers either in a one-pot reaction[7] or in two separate steps.[8] Throughout a series of preliminary experiments, we noticed that solvothermal reactions of Zn^{2+} and aromatic dicarboxylic acid in DMF predominantly produce 2D layered structures based on "paddle-wheel" units.[9] With solvent molecules occupying both ends of the dinuclear center this type of charge-neutral 2D layers would be ideal candidates to pillar, and therefore, we set out to construct 3D open frameworks by using linear connectors along with Zn^{2+} and dicarboxylic acid. Unsuccessful attempts include the use of pyrazine or 1,4-dicyanobenzene which, in the presence of DMF as the solvent, does not bridge between two Zn^{2+} ions. When dabco was used as the pillaring agent, however, we obtained a 3D framework with expected connectivity, and the porous and dynamic nature of the framework $[Zn_2(1,4\text{-bdc})_2(dabco)]$ (**1**) has recently been reported.[5a] Following this lead, we examined a series of isomorphous frameworks by a systematic modulation of **1**, and open frameworks **2**–**8** were obtained.

The synthesis involves heating a solution of the reactants, typically in DMF or in a MeOH/DMF mixture, to 90–120 °C in a closed vessel. The reactions are reproducible, and can be readily scaled up to produce a gram quantity of crystalline products. The structures were deduced by X-ray crystallographic analysis on single crystals, and powder diffraction patterns of bulk samples were compared to their simulations based on single-crystal structures to confirm the phase purity (see Supporting Information). No secondary phase was observed in any of the reaction products described above for **2**–**8**.

Frameworks **2** and **3** are derived by a partial or complete, respectively, replacement of 1,4-bdc in **1** with tmbdc (Figure 1a and b). The methyl groups of tmbdc reduce the size of windows, which are already smaller than those in **1** due to a non-zero dihedral angle between phenyl and carboxylate planes (75.0(1)° for **2** and 73.9(1)° for **3**). Therefore, the pore structure of **3** is characterized by cavities measuring 6–8 Å interconnected through 3.5 Å windows. The free volume in **3**, estimated from the crystal structure (30%), is far underestimated due to the two-fold conformational disorder in tmbdc linkers. Considering that **1** has a solvent-accessible free volume of approximately 62%, the void volume in the crystals of **2** and **3** is expected to be in the range of 45–55%. It is noted that the formation of **3** contradicts a previous belief[10] that tmbdc does not allow a square-grid net based on paddle-wheel units for steric reasons. We assume that alternating orientations of phenyl

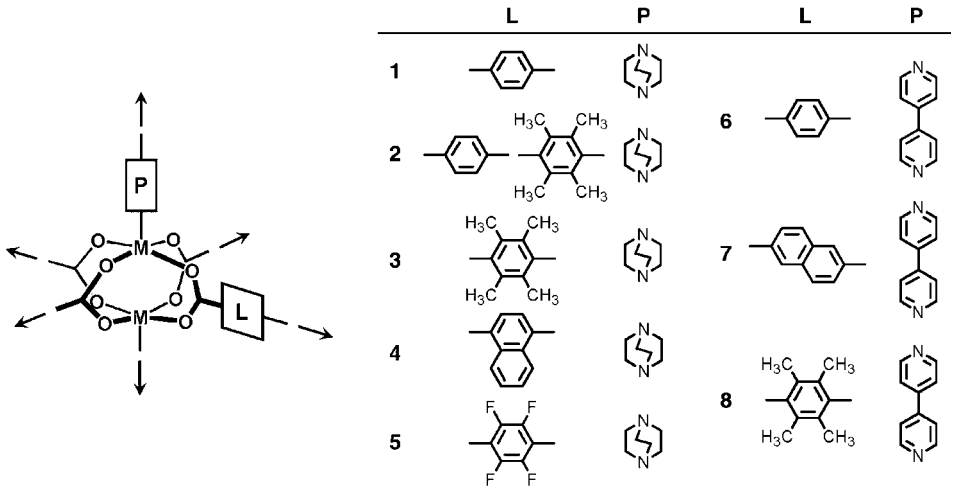

Scheme 1. Linkers (L) and pillars (P) in paddle-wheel-based nets **1**–**8**.

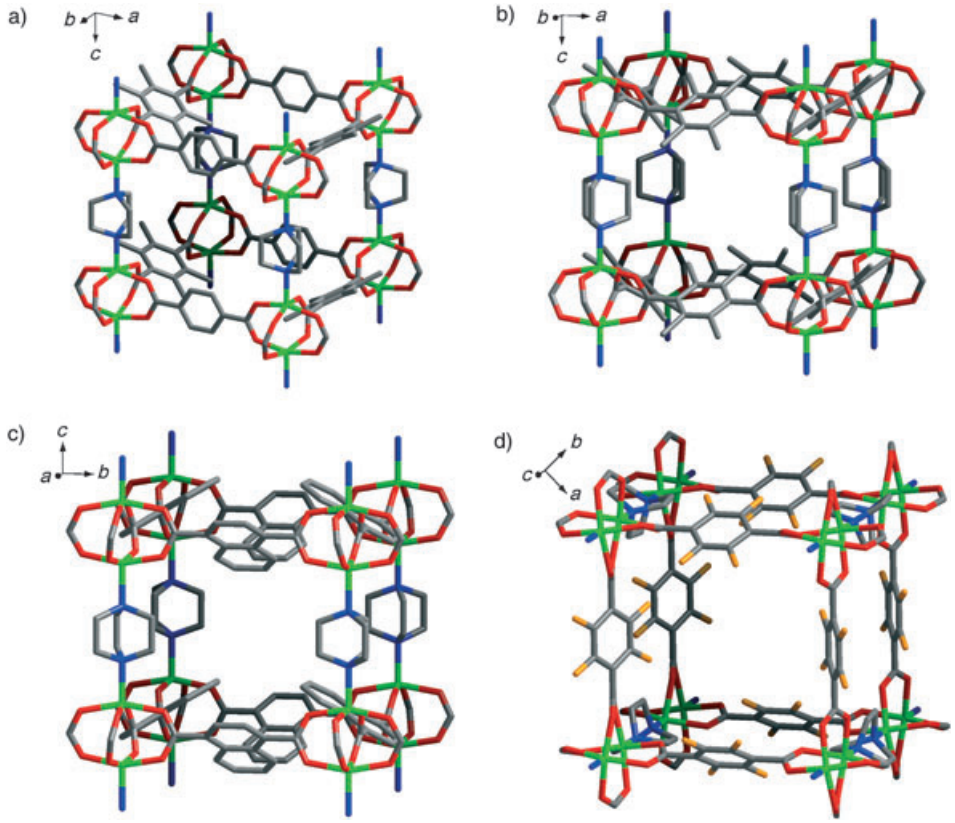

Figure 1. Partially expanded structures of a) **2**, b) **3**, c) **4** and d) **5** showing cube-like cages. For a)–c), dicarboxylate linkers are disordered and only one of the possible conformations is shown. Hydrogen atoms are omitted. Color code: Zn: green; N: blue; O: red; C: gray; F: orange.

rings around a square of four paddle-wheels renders enough space to accommodate the methyl groups. As a consequence, the tmbdc linkers are conformationally disordered over two positions in the crystal structures of **2** and **3**, and in the case of **2**, 1,4-bdc and tmbdc statistically occupy the same positions (see Supporting Information). The refined site occupancy factors of 1,4-bdc and tmbdc in the X-ray structure converged to a value close to equal contributions from each component. More directly, the 1:1 stoichiometry of 1,4-bdc and tmbdc in **2** has been established by a ^{1}H NMR measurement of the product dissolved in NaOH/D_2O solution, in which three singlets are observed with expected chemical shifts in a ratio of 1:3:3 for the protons of 1,4-bdc, dabco, and tmbdc, respectively.

Aromatic substituents on the phenyl ring of 1,4-bdc may play a different role from that of alkyl substituents in gas sorption, and therefore, 1,4-naphthalenedicarboxylate (1,4-ndc) was used in place of 1,4-bdc to obtain an isomorphous framework **4** (Figure 1c). Although the naphthalene moiety of 1,4-ndc is disordered in a way similar to tmbdc in **3** (see Supporting Information), the overall connectivity and the underlying topology of **4** are unambiguously defined to be the same as those of **1**–**3**. Again, without alternating orientations of the naphathalene moieties in a square of four paddle-wheel units the steric hindrance would have not allowed the formation of **4**. The dihedral angle between carboxylate and aromatic planes (69.2(1)°) is somewhat smaller than that for tmbdc in **2** and **3**. Structural characteristics, such as pore size, channel shape, and free volume of **4** are as expected not much different from those of **3** except for the nature of the chemical functionality. For instance, frameworks **3** and **4** have an equal number of extra carbon atoms in the backbone compared to **1**, whereas they are one half in **2**. Therefore, if the side groups of the 1,4-bdc derivatives are inactive towards gas sorption, then the decrease in the surface area in **3** and **4** from **1** should be similar and significantly larger than in **2**.

Of particular curiosity for us during this systematic modulation process was whether an electronic factor plays a role in the physisorption of gas although this was counterintuitive. Therefore, we decided to use a tetrahalo-substituted linker, and a simple geometric consideration was enough to realize that tetrabromo- or tetrachloro-substituted 1,4-bdc are sterically too demanding for a paddle-wheel-based square grid net since the dihedral angle between the phenyl ring and carboxylate plane should be nearly 90°. Consequently, we focused our efforts on the synthesis of an isomorphous framework with tetrafluoroterephthalic acid (H_2tfbdc). The product thus obtained was formulated as $[Zn_2(tfbdc)_2(dabco)]$ (**5**) based on X-ray crystallographic analysis on a single crystal which was completely evacuated prior to the diffraction measurements.[11] The difference Fourier map after final refinements of the framework atoms is virtually flat,[12] and the solvent-accessible voids in the crystal are estimated to account for 55% of the crystal volume, with the simultaneous occupation of all disordered sites of dabco ligands. Unlike **2**–**4**, the dicarboxylate linker in the crystal structure of **5** (Figure 1d) is conformationally ordered, and the dihedral angle between the phenyl ring and carboxylate plane is 44.4(3)°. The fully ordered, alternating orientations of tetrafluorophenyl moieties around a square in **5** verify the simple geometric requirement to accommodate the side groups of the 1,4-bdc derivatives in **2**–**4** discussed above. A Cu^{II} analogue of **5** and its structure based on X-ray powder diffraction analysis was published at the time of writing this paper.[8a] The structure of the Cu^{II} framework in the report is similar to that of **5** except for the

fact that the structure was defined in space group *P*4/*mmm* where the tfbdc linker should have been conformationally disordered. The crystal structure of **5** is best described in space group *P*4/*nbm* with a unit cell volume twice that of *P*4/*mmm*. Note that setting the space group for **2**–**4** to *P*4/*nbm* with a doubled unit cell volume does not make the dicarboxylate linkers ordered: they are inherently disordered. Each of the cavity-like pores in **5** is equivalent to others; four tfbdc units point inward and four outward. The channels along the *c* axis have a free passage of 6 Å, and the cavity surrounded by eight paddle-wheel units measures 7.5×11 Å^2 considering the van der Waals surface of the framework atoms. The volume of the cavity-like pore (633 Å^3) is equivalent to approximately 15 hydrogen-bonded water molecules. For comparison, **1** has straight channels with a 7.5-Å opening and an internal diameter of 10–11 Å. The free volume per cavity of **1** of 708 Å^3 is also somewhat larger than that of **5**. Figure 2 compares the solvent-accessible surface of derivatized frameworks **3** and **5** to their parent net **1**, and clearly shows the changes in pore environments caused by the extra functional groups. From the gas-sorption point of view, **5** has a disadvantage compared to **1** not because of the slightly reduced pore size, but because of its higher framework density originating from the fluorine atoms. The densities for **5** and **1** based on crystallographic analysis are 1.034 and 0.826 g cm^{-3}, respectively.

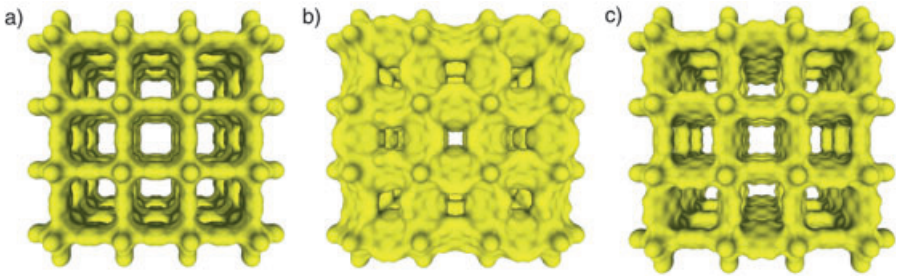

Figure 2. Solvent-accessible surface (1.4 Å probe radius) of a) **1**, b) **3**, c) **5** viewed down the *c* axis. Effective openings along the *a* and *b* directions measure 3.5×5 Å^2.

In an effort to obtain an isomorphous net with a framework density lower and surface area higher than **1**, we tried to replace 1,4-bdc and dabco ligands in **1** with 2,6-ndc and bpy, respectively. This natural expansion of the series led to the successful isolation of $[Zn_2(1,4\text{-bdc})_2(bpy)]$ (**6**) and $[Zn_2(2,6\text{-ndc})_2(bpy)]$ (**7**) where the network topology is exactly as expected (Figure 3a and c). The pores of the expanded nets, however, are found to be too large for a dinuclear paddle-wheel node, and not surprisingly, two- and threefold interpenetrations by the same net are observed in **6** and **7**, respectively (Figure 3b and d). A Cu^{II} analogue of **6**, and its characterization by X-ray powder diffraction and gas sorption studies have previously been reported.[13] Meanwhile, the threefold interpenetration in **7** eliminates most of the void space in the structure, and therefore it was not studied further for gas sorption.

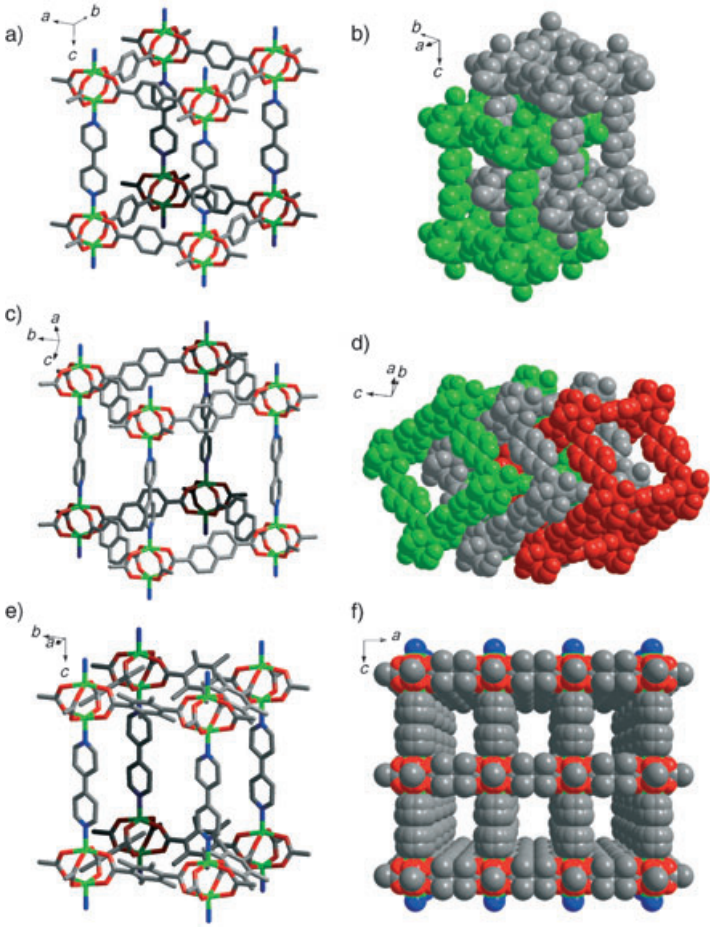

Figure 3. Crystal structures of frameworks **6** (a,b), **7** (c,d), and **8** (e,f) after a partial expansion. Two- and threefold interpenetrations observed in **6** and **7** are shown in (b) and (d), respectively. f) Perspective view of **8** down the *b* axis. All the possible conformations of disordered tmbdc and bpy ligands are shown.

We thought that by using a derivative of 1,4-bdc the interpenetration observed in **6** could be avoided by reducing the size of pores and free apertures along the *c* direction. Therefore, H_2tmbdc was used along with bpy in the same synthetic protocol. This resulted in a non-interpenetrating 3D framework $[Zn_2(tmbdc)_2(bpy)]$ (**8**). Again, the overall connectivity and underlying topology of **8** are the same as the rest of the frameworks, as shown in Figure 3e. Compared to the parent net **1**, in which the largest opening is along the *c* axis, the open structure of **8**, which has large pores measuring 8×10 Å^2, allows a maximum free-passage of 7.5 Å in the *a* or *b* direction, whereas the window in the *c* direction (3.5 Å) is partially blocked by tetramethylphenyl moieties as in the case of **3**. In terms of the cavity size, **3** and **8** share the same dimensions except for the length of the pillar, and the dis-

tance between two nearest zinc ions separated by the pillaring ligand is 6.7 and 11.1 Å in **3** and **8**, respectively. The structural relationship between **8** and **3**, and between **3** and other frameworks will be important in analyzing gas sorption properties. Both the tmbdc linker and the bpy pillar in **8** are rotationally disordered, and the solvent-accessible voids in the structure calculated after allowing simultaneous occupations of all disordered sites account for 48% of the crystal volume. Framework **8** has a crystallographic density (0.731 $g\,cm^{-3}$) lower than that of **1**, while they share the same connectivity and topology, and therefore it would be interesting to see whether the lower framework density leads to a higher surface area.

Results of the thermogravimetric analysis (TGA) for frameworks **2**–**5** and **8** measured under a N_2 atmosphere are shown in Figure 4. The observed weight losses for **3** (25.7%)

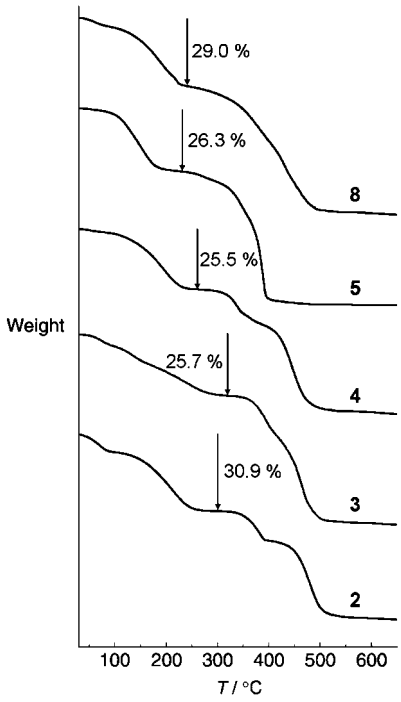

Figure 4. TGA plots of porous frameworks **2**–**5** and **8** recorded under an N_2 atmosphere. All the samples are as-synthesized except for **5** which was soaked in DMF overnight prior to the measurement.

and **4** (25.5%) are reasonably close to calculated values based on elemental analysis (27.2% for **3** and 27.6% for **4**). For others, such a comparison is not made since the exact amount of guests in as-synthesized samples is unknown due to severe disorder in X-ray structures and inconsistent elemental analysis. In principle, TGA measurements alone cannot be used to determine the stability of an open structure since it may collapse without a notable change in the weight. However, the data in Figure 4 suggest that the porous nets in this study have a stability range 200–320 °C under an inert atmosphere. X-ray powder diffraction analyses carried out for the evacuated solids confirm the stability of the open structures in the absence of guest molecules (Figure 5). For **3**, X-ray diffraction patterns were measured at different temperatures to unambiguously establish the

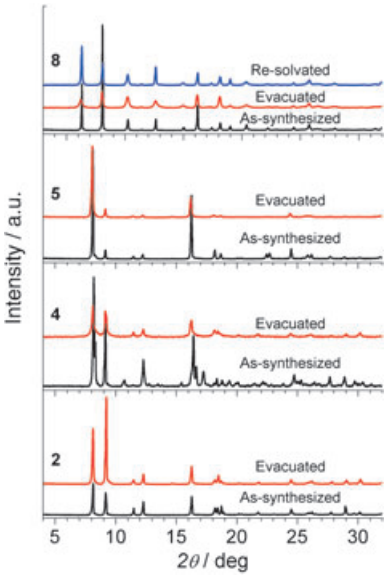

Figure 5. X-ray powder diffraction patterns for as-synthesized and evacuated samples of **2**, **4**, **5**, and **8** measured at room temperature. The evacuation was carried out by heating to 120 °C under vacuum for 12 h.

stability of its bulk phase. The fully evacuated open structures have been found to be stable at least up to 200 °C in air (Figure 6). Note that there is an unusual line broadening

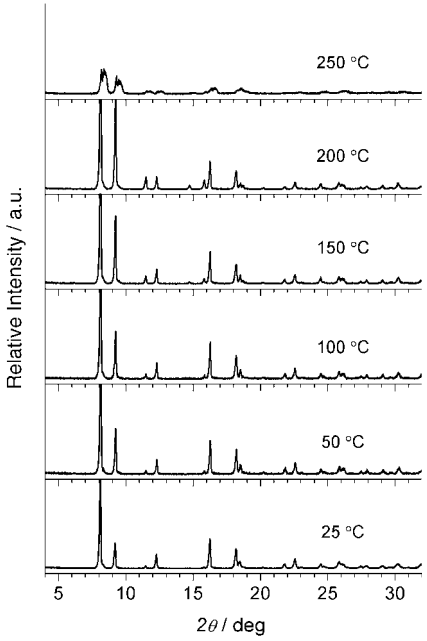

Figure 6. Temperature progression of X-ray powder diffraction patterns for **3** measured in air. The sample was held at designated temperatures for at least 30 min.

in the diffraction pattern of **8** after complete evacuation (Figure 5). A collapse of the framework can be ruled out since the peaks reversibly sharpen as the sample gets re-solvated. Instead, we suspect that an unknown dynamic property exists in the evacuated structure owing to the increased length of the pillar that supports the porous network without interpenetration. Nevertheless, **8** displays permanent porosity and a high surface area, as we will show below with gas sorption data. Notably, from Figure 5 and 6, none of the frameworks show the dynamic behavior observed in **1**[5a] upon the inclusion and removal of guest molecules in the pores.

Gas sorption properties: The porosity and specific surface areas of framework materials **2–5** and **8** were estimated by measuring nitrogen gas sorption isotherms at 78 K. The sorption of hydrogen gas has also been studied under the same conditions. The isotherms are shown in Figure 7, and the results of the analysis are summarized in Table 1.

In all cases the sorption of nitrogen reaches near-saturation at low relative pressures ($P/P_0 < 0.05$) and thereafter increases very slowly up to 1 atm. These are type I isotherms typical for a microporous material. There is no significant hysteresis between sorption and desorption traces (see the Supporting Information). The total pore volume (Table 1), which is the volume adsorbed at STP when P/P_0 approaches 1, ranges from 0.45 (**8**) to 0.59 $cm^3 cm^{-3}$ (**5**). Although smaller than that of **1** (0.62 $cm^3 cm^{-3}$), the numbers compare favorably with those of most zeolites ($\leq$ 0.50 $cm^3 cm^{-3}$).[14] With an approximation based on a monolayer condensation of adsorbed N_2 molecules on a uniform surface, the sorption isotherms were fitted to a Langmuir equation and gave surface areas for the derivatized frameworks from 1400 (**8**) to 1740 $m^2 g^{-1}$ (**2**). The same calculations for unmodified framework **1** gave a Langmuir surface area of 2090 $m^2 g^{-1}$.

Introduction of substituents on the phenyl ring of 1,4-bdc results in a significant decrease in the surface area of **2–5** with respect to that of **1**, which may be easily understood and expected from the crystal structures. The increase in the surface area as well as in the number of adsorbed N_2 molecules per formula unit of **8** compared to that of **3** is viewed in the same context. However, the chemical nature of the side groups of the 1,4-bdc derivatives (aliphatic (**3**), aromatic (**4**), or halogenic (**5**)) appears to be irrelevant with regard to the trends observed.

The shape of the H_2 sorption isotherms shown in Figure 7 is typical for their kind,[5] and is attributed to the fact that the temperature (−196 °C) is well above the boiling point of hydrogen (−253 °C at 1 atm). The sorption and desorption curves almost overlap for **1–3**; however, a marked hysteresis is observed for **4** and to a lesser degree for **5** and **8** (see the Supporting Information). We cannot correlate the observed hysteresis with pore structures of corresponding frameworks (Figure 2) at the moment; however, such behavior may be

Table 1. Summary of N_2 and H_2 gas sorption data.

	A [$m^2 g^{-1}$] Langmuir (BET)	V_p [$cm^3 g^{-1}$] ([$cm^3 cm^{-3}$])	N_2 per f.u.[a]	H_2 at 1 atm [$cm^3 g^{-1}$] ([$mg g^{-1}$])	H_2 per f.u.[a]	Relative surface coverage by H_2 [%] (V_{occ} [%])[b]
1	2090 (1450)	0.75 (0.62)	12.3	223 (20.1)	5.7	36.6 (37.7)
2	1670 (1100)	0.59 (0.54)	10.7	230 (20.8)	6.5	47.5 (49.7)
3	1400 (920)	0.50 (0.50)	9.9	205 (18.5)	6.2	50.3 (52.2)
4	1450 (1000)	0.52 (0.50)	10.1	189 (17.0)	5.7	44.8 (46.0)
5	1610 (1070)	0.57 (0.59)	11.9	197 (17.8)	6.3	42.0 (44.0)
8	1740 (1120)	0.62 (0.45)	13.0	187 (16.8)	6.1	36.9 (38.2)

[a] Formula unit (f.u.), [Zn_2(dicarboxylate)$_2$(diamine)]. [b] Percentage of pore volume ($cm^3 g^{-1}$) occupied by adsorbed H_2 which is assumed to have liquid density at 1 atm and boiling point (70.973 $kg m^{-3}$).

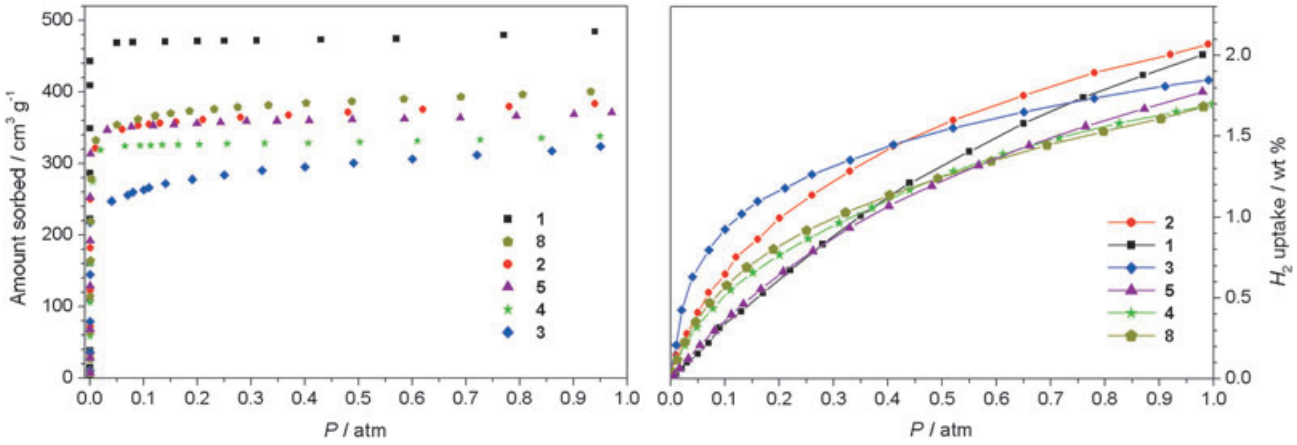

Figure 7. N_2 (left) and H_2 (right) gas sorption isotherms of **2–5** and **8** measured at 78 K. Data for **1** are shown for comparison. The N_2 isotherms are reversible without a significant hysteresis between sorption and desorption curves, whereas H_2 isotherms of **4** display some hysteresis (see Supporting Information). Solid lines in H_2 isotherms are visual aids.

of interest since it allows H_2 to be stored at a pressure lower than when it is charged.[15]

A characteristic feature that is clearly apparent from the H_2 sorption isotherms shown in Figure 7 is the different slopes of the curves in the low pressure ranges ($P < 0.4$ atm). For example, **3**, in which 1,4-bdc is completely replaced by tmbdc, shows the fastest rise in H_2 uptake, whereas the initial slope of **1** is the flattest in the series. It may not be a coincidence that free apertures in the structures of **3** and **1** are the smallest and largest, respectively, among the isomorphous frameworks. The free channels in **1** along the *c* axis are uniform and straight with the diameter of 7.5 Å, whereas those of **3** have several indentations with the narrowest part being barely over 3 Å. In general, the lower pressure range ($P/P_0 \leq 0.3$) in BET isotherms is considered as the region where gas molecules cover the surface almost exclusively as a monolayer. Therefore, it may be said that the affinity of H_2 molecules towards the frameworks in this study is the highest for **3**, intermediate for **2**, **4**, and **8**, and lowest for **1** and **5**. We believe that the shape and size of channels, rather than the chemical nature of organic linkers, are responsible for this trend. Further support for this argument is available from the similar values of sorbed H_2 at 1 atm, 187–230 $cm^3 g^{-1}$ or 1.7–2.1 wt %,[16] which become more uniform when translated into molecular terms, such as the number of sorbed H_2 molecules per paddle-wheel unit (from 5.7 H_2 for **1** and **4** to 6.5 H_2 in **2**). The lack of differences consequently leads to a relative surface coverage by H_2[17] which is in an approximately reverse order to that of the surface area determined by N_2 sorption experiments. Thus, similar to our analysis on the surface affinity, **3** and **1** have the most and least effective surface coverage with 50 and 37 %, respectively. The fraction of pore volume occupied by adsorbed H_2 may be an alternative representation of the relative surface coverage by H_2, and the values for frameworks **1**–**5** and **8** are in good agreement (the last column of Table 1).

Taken together with studies on other metal-organic open frameworks,[5] it appears that some metal-organic frameworks possess higher affinity towards H_2 than other frameworks, and we believe that they are the ones with wavy channels and limited size of free passage rather than those with straight channels and large openings. This conjecture, which is derived from the analysis of experimental data, is consistent with a theoretical study on methane sorption[18] that considers the heat of adsorption, which is higher in smaller pores, as an index of energetic interaction between sorbate and sorbent. Another theoretical study on a metal-organic framework[19] having two kinds of pores also suggests that the preferred adsorption site for argon is smaller pores. The ultimate capacity for H_2 storage, on the other hand, should also be related to available surface area, since a "pore-filling" effect will become significant under high pressure conditions. This is also evident from the H_2 sorption isotherm of **3**, which has the highest initial slope but already begins to saturate in the given pressure range. Therefore, an ideal porous material intended for storing hydrogen gas through physisorption would have to possess a large surface area, high void fraction, sinuous channels with a curvature and free windows of limited size. Based on our data and those in literature, we propose that a porous material with the surface area of 2000 $m^2 g^{-1}$ or above, a void fraction of 60 % or more, and free windows of 6 Å or less may show an unprecedented H_2 storage capacity. We believe that it is not impossible to meet the first and the last requirements within the same material, and our current effort is focused on new metal-organic frameworks to realize this goal.

Conclusion

We have successfully synthesized and fully characterized a series of 3D metal-organic frameworks in which dinuclear paddle-wheel units are connected by linear linkers and diamine pillars. The metal–dicarboxylate–diamine system allows a systematic modulation of either or both the linkers and pillars without changing the α-Po topology, that is, the change can be made anisotropically. Gas sorption studies reveal that the closely related materials possess a permanent porosity in terms of reversible gas sorption and high surface area. The aromatic (1,4-ndc in **4**) or electron-withdrawing groups of the dicarboxylate linker (tfbdc in **5**) have not been found to exert a favorable influence on the physisorption of N_2 or H_2 gas molecules. The amounts of nitrogen sorption and the surface areas determined from it do not depart greatly from expectations based on the crystal structures. In the case of hydrogen, however, framework **3**, which has the most crowded pore environment, shows the highest affinity towards the gas at low pressures, and the sorption capacities of related materials measured at 1 atm do not directly mirror the available surface areas judging from the similar numbers of sorbed H_2 molecules per formula unit. Therefore, as a hydrogen-storage material we suggest preference should be given to a system in which small windows and sinuous channels lead to a high surface area. This conclusion helps to better understand the physisorption of gases in metal-organic frameworks and should help to design new porous materials with an efficient hydrogen-storage capacity.

Experimental Section

General considerations: All the ligands and transition metal salts were obtained commercially and used as received. TGA data were obtained on a Perkin-Elmer Pyris 1 TGA instrument with a heating rate of 10 °C min^{-1} under a N_2 atmosphere. The X-ray powder diffraction patterns were recorded on a Bruker D8 Avance system equipped with a Cu sealed tube ($\lambda = 1.54178$ Å) at a scan rate of 10 s deg^{-1}. BET gas sorption isotherms were measured with a custom-made vacuum manifold following a standard volumetric technique at 78 K. The hydrogen gas used was purchased from BOC Gases Korea and was of high purity (99.999 %). Typically, a sample of as-synthesized material (150–200 mg) was loaded and, prior to the measurements, evacuated by heating to 120 °C under a high vacuum (10^{-5} torr) overnight. For **5** and **8**, the evacuation was carried out at room temperature after exchanging the guests with $CHCl_3$.

Synthesis of $[Zn_2(1,4\text{-bdc})(tmbdc)(dabco)]$ (2): dabco (6 mg, 0.05 mmol) was added to a solution containing H_2tmbdc (11 mg, 0.05 mmol), H_2bdc (8 mg, 0.05 mmol) and $Zn(NO_3)_2{\cdot}6H_2O$ (30 mg, 0.1 mmol) in DMF (1.5 mL), and the resulting slurry was stirred at room temperature for 3 h. After the white precipitate had been filtered off by gravity, the solution was heated to 120 °C in a sealed glass tube for two days to produce colorless, brick-shaped crystals (27 mg). The product was washed with DMF and dried at 105 °C under vacuum overnight to obtain an evacuated framework (20 mg, 63 %). A portion of the desolvated solid was added to NaOH in D_2O and subjected to ^{1}H NMR measurements. ^{1}H NMR (500 MHz, D_2O, 25 °C, TMS): $\delta = 7.80$ (4H; bdc), 2.65 (12.2H; dabco), 2.06 ppm (11.8H; tmbdc). Elemental analysis was carried out for evacuated samples because of inconsistent results from as-synthesized materials. Elemental analysis calcd (%) for $[Zn_2(1,4\text{-bdc})(tmbdc)(dabco)]{\cdot}3H_2O$ (681.32): C 45.84, H 5.03, N 4.11; found: C 45.54, H 4.59, N 4.41.

Synthesis of $[Zn_2(tmbdc)_2(dabco)]$ (3): H_2tmbdc (140 mg, 0.63 mmol), $Zn(NO_3)_2{\cdot}6H_2O$ (189 mg, 0.63 mmol) and dabco (35 mg, 0.31 mmol) were mixed in DMF (15 mL) and homogenized by stirring for 2 h. The slurry was heated to 120 °C in a Teflon-lined stainless still bomb reactor for 32 h to obtain a white microcrystalline precipitate (275 mg, 93 %). Single crystals for structural study were obtained by following the same procedure described above for **2**. Elemental analysis calcd (%) for as-synthesized material $[Zn_2(tmbdc)_2(dabco)]{\cdot}3DMF{\cdot}2H_2O$ (938.70): C 49.90, H 6.55, N 7.46; found C 49.39, H 6.70, N 7.82.

Synthesis of $[Zn_2(1,4\text{-ndc})_2(dabco)]$ (4): The standard protocol described above for **2** was employed, and brick-shaped crystals with greenish yellow color were obtained in 76 % yield. Elemental analysis calcd (%) for as-synthesized material $[Zn_2(1,4\text{-ndc})_2(dabco)]{\cdot}3DMF{\cdot}2H_2O$ (926.60): C 50.55, H 5.33, N 7.56; found: C 50.62, H 5.32, N 7.86.

Synthesis of $[Zn_2(tfbdc)_2(dabco)]$ (5): $Zn(NO_3)_2{\cdot}6H_2O$ (119 mg, 0.40 mmol) and H_2tfbdc (96 mg, 0.40 mmol) were dissolved in methanol (5 mL). After dabco (22 mg, 0.20 mmol) and DMF (1.2 mL) were added to the mixture, it was stirred for 1 h at room temperature, and then a white precipitate was filtered off. The resulting solution, upon heating to 95 °C for 7 h, produced colorless, brick-shaped crystals. The product (105 mg) was washed with DMF and methanol and heated to 95 °C under vacuum overnight to give evacuated framework (79 mg, 55 %). C,H,N analysis was carried out for evacuated samples. Elemental analysis calcd (%) for $[Zn_2(tfbdc)_2(dabco)]{\cdot}2H_2O$ (751.12): C 35.18, H 2.15, N 3.73; found: C 35.62, H 2.69, N 4.07.

Synthesis of $[Zn_2(1,4\text{-bdc})_2(bpy)]$ (6): $Zn(NO_3)_2{\cdot}6H_2O$ (89 mg, 0.30 mmol) and H_2bdc (50 mg, 0.30 mmol) were dissolved in a mixture of MeOH and DMF (1:1, 6 mL). Addition of bpy (23 mg, 0.15 mmol) to the mixture led to formation a white slurry. The heterogeneous mixture was stirred at room temperature for 24 h and heated to 120 °C in a closed vessel for two days. A microcrystalline precipitate was isolated, thoroughly washed with DMF, and dried in vacuo (85 mg, 92 %). Single crystals for structural study were obtained from the same reaction in a DMF/xylene mixed solvent. Elemental analysis calcd (%) for evacuated solid $[Zn_2(1,4\text{-bdc})_2(bpy)]$ (615.15): C 50.76, H 2.62, N 4.55; found C 50.43, H 2.75, N 4.89.

Synthesis of $[Zn_2(2,6\text{-ndc})_2(bpy)]$ (7): The same procedure as that for **6** was used for this compound except for the use of H_2(2,6-ndc) instead of H_2bdc. The yield was nearly quantitative. Elemental analysis calcd (%) for $[Zn_2(2,6\text{-ndc})_2(bpy)]{\cdot}0.5DMF{\cdot}H_2O$ (769.86): C 55.39, H 3.34, N 4.55; found: C 55.16, H 3.04, N 4.58.

Synthesis of $[Zn_2(tmbdc)_2(bpy)]$ (8): This compound was obtained as colorless block-shaped crystals by following the same procedure as that for **2**. The as-synthesized product was guest-exchanged with $CHCl_3$ and evacuated under vacuum at room temperature. The yield was nearly quantitative. Elemental analysis calcd (%) for $[Zn_2(tmbdc)_2(bpy)]{\cdot}2H_2O$ (763.43): C 53.49, H 4.75, N 3.67; found: C 53.60, H 4.85, N 4.32.

Crystal structure determination: Single crystals were picked up with paraton oil on the tip of a glass fiber and mounted on a Siemens SMART CCD diffractometer equipped with a graphite-monochromated $Mo_{K\alpha}$ ($\lambda = 0.71073$ Å) radiation source in a cold nitrogen stream. For **2**, **4**, and **5** diffraction data were collected for both as-synthesized and evacuated crystals, and only the latter are reported here. For **3** and **8**, contributions from disordered solvent molecules were removed by the SQUEEZE routine (PLATON),[20] and the outputs from the SQUEEZE calculations are attached to each CIF file. All crystallographic data were corrected for Lorentz and polarization effects (SAINT), and semiempirical absorption corrections based on equivalent reflections were applied (SADABS). The structures were solved by direct methods and refined by the full-matrix least-squares method on F^2 with appropriate software implemented in the SHELXTL program package. All the non-hydrogen atoms except for those of disordered solvent molecules in **6** were refined anisotropically with least-squares restraints, when necessary. Hydrogen atoms were added at their geometrically ideal positions. Conformationally disordered ligands were treated with split-atom models. Crystal data and results of the structure refinements are summarized in Table 2 and Table 3. CCDC 255610–CCDC-255616 (**2**–**8**) contain the supplementary crystallographic data for this paper. These data can be obtained free of charge from The Cambridge Crystallographic Data Centre via www.ccdc.cam.ac.uk/data_request/cif.

Acknowledgements

We gratefully acknowledge the Creative Research Initiative Program of the Korean Ministry of Science and Technology for support of this work and the BK 21 Program of the Korean Ministry of Education for a graduate studentship to H. K.

Table 2. Summary of crystal data and structure refinements for porous frameworks **2**–**5** and **8**.

	2	**3**	**4**	**5**	**8**
formula	$C_{26}H_{28}N_2O_8Zn_2$	$C_{30}H_{36}N_2O_8Zn_2$	$C_{30}H_{24}N_2O_8Zn_2$	$C_{22}H_{12}F_8N_2O_8Zn_2$	$C_{34}H_{32}N_2O_8Zn_2$
FW	627.24	683.35	671.25	715.08	727.36
T [K]	223	213	297	223	223
crystal system	tetragonal	tetragonal	tetragonal	tetragonal	tetragonal
space group	*P*4/*mmm*	*P*4/*mmm*	*P*4/*mmm*	*P*4/*nbm*	*P*4/*mmm*
a [Å]	10.895(1)	10.869(1)	10.921(1)	15.451(1)	10.877(1)
c [Å]	9.569(1)	9.563(3)	9.611(1)	9.620(1)	13.964(3)
V [Å^3]	1135.9(2)	1129.7(4)	1146.3(1)	2296.5(2)	1652.1(4)
Z	1	1	1	2	1
ρ_{calcd} [g cm^{-3}]	0.917	1.004	0.972	1.034	0.731
μ [mm^{-1}]	1.086	1.096	1.080	1.105	0.752
T_{max}/T_{min}	0.8717/0.7295	0.9472/0.8797	0.6422/0.6143	0.7696/0.6361	0.8641/0.8227
reflections measured	6719	4788	6507	11379	7819
independent (R_{int})	816 (0.0459)	527 (0.0994)	885 (0.0351)	1249 (0.0433)	888 (0.0789)
restraints/parameters	6/63	6/57	25/81	24/80	6/69
GOF	1.421	1.066	1.334	1.094	1.104
R_1, wR_2 [$I > 2\sigma(I)$]	0.0465, 0.1559	0.0585, 0.1610	0.0491, 0.1638	0.0364, 0.0963	0.0536, 0.1389
R_1, wR_2 (all data)	0.0483, 0.1572	0.0668, 0.1652	0.0500, 0.1650	0.0478, 0.1085	0.0612, 0.1429
ρ_{max}/ρ_{min} [e Å^{-3}]	0.906/−0.530	1.195/−0.624	1.261/−0.695	0.656/−0.771	1.283/−1.005

Table 3. Summary of crystal data and structure refinements for interpenetrated frameworks **6** and **7**.

	6	**7**
formula	$C_{26}H_{16}N_2O_8Zn_2$	$C_{34}H_{20}N_2O_8Zn_2$
FW	615.15	715.26
T [K]	243	223
crystal system	triclinic	monoclinic
space group	$P\bar{1}$	$C2/m$
a [Å]	10.883(1)	10.458(3)
b [Å]	10.926(1)	19.896(7)
c [Å]	14.066(2)	7.753(2)
α [°]	92.417(2)	90
β [°]	90.099(2)	100.07(3)
γ [°]	101.723(2)	90
V [Å^3]	1636.1(3)	1588.5(8)
Z	2	2
ρ_{calcd} [g cm^{-3}]	1.249	1.495
μ [mm^{-1}]	1.507	1.564
T_{max}/T_{min}	0.7526/0.6606	0.8593/0.7450
reflections measured	9742	3506
independent (R_{int})	7306 (0.0328)	1284 (0.0639)
restraints/parameters	0/359	0/79
GOF	1.093	1.224
R_1, wR_2 [$I>2\sigma(I)$]	0.0776, 0.1950	0.1147, 0.2663
R_1, wR_2 (all data)	0.1019, 0.2121	0.1453, 0.2801
ρ_{max}/ρ_{min} [e Å^{-3}]	1.435/−1.286	1.317/−1.217

[1] a) S. Kitagawa, R. Kitaura, S.-i. Noro, *Angew. Chem.* **2004**, *116*, 2388–2430; *Angew. Chem. Int. Ed.* **2004**, *43*, 2334–2375; b) C. N. R. Rao, S. Natarajan, R. Vaidhyanathan, *Angew. Chem.* **2004**, *116*, 1490–1521; *Angew. Chem. Int. Ed.* **2004**, *43*, 1466–1496; c) O. M. Yaghi, M. O'Keeffe, N. W. Ockwig, H. K. Chae, M. Eddaoudi, J. Kim, *Nature* **2003**, *423*, 705–714; d) S. L. James, *Chem. Soc. Rev.* **2003**, *32*, 276–288; e) C. Janiak, *Dalton Trans.* **2003**, 2781–2804; f) M. Eddaoudi, D. B. Moler, H. Li, B. Chen, T. M. Reineke, M. O'Keeffe, O. M. Yaghi, *Acc. Chem. Res.* **2001**, *34*, 319–330.

[2] a) H. Li, M. Eddaoudi, T. L. Groy, O. M. Yaghi, *J. Am. Chem. Soc.* **1998**, *120*, 8571–8572; b) S. S.-Y. Chui, S. M.-F. Lo, J. P. H. Charmant, A. G. Orpen, I. D. Williams, *Science* **1999**, *283*, 1148–1150; c) H. Li, M. Eddaoudi, M. O'Keeffe, O. M. Yaghi, *Nature* **1999**, *402*, 276–279.

[3] M. Eddaoudi, J. Kim, N. Rosi, D. Vodak, J. Wachter, M. O'Keeffe, O. M. Yaghi, *Science* **2002**, *295*, 469–472.

[4] a) R. F. Service, *Science* **2004**, *305*, 958–961; b) L. Schlapbach, A. Züttel, *Nature* **2001**, *414*, 353–358.

[5] a) D. N. Dybtsev, H. Chun, K. Kim, *Angew. Chem.* **2004**, *116*, 5143–5146; *Angew. Chem. Int. Ed.* **2004**, *43*, 5033–5036; b) E. Y. Lee, M. P. Suh, *Angew. Chem.* **2004**, *116*, 2858–2861; *Angew. Chem. Int. Ed.* **2004**, *43*, 2798–2801; c) J. L. C. Rowsell, A. R. Millward, K. S. Park, O. M. Yaghi, *J. Am. Chem. Soc.* **2004**, *126*, 5666–5667; d) L. Pan, M. B. Sander, X. Huang, J. Li, M. Smith, E. Bittner, B. Bockrath, J. K. Johnson, *J. Am. Chem. Soc.* **2004**, *126*, 1308–1309; e) D. N. Dybtsev, H. Chun, S. H. Yoon, D. Kim, K. Kim, *J. Am. Chem. Soc.* **2004**, *126*, 32–33; f) G. Férey, M. Latroche, C. Serre, F. Millange, T. Loiseau, A. Percheron-Guégan, *Chem. Commun.* **2003**, 2976–2977; g) N. L. Rosi, J. Eckert, M. Eddaoudi, D. T. Vodak, J. Kim, M. O'Keeffe, O. M. Yaghi, *Science* **2003**, *300*, 1127–1129; h) P. M. Forster, J. Eckert, J.-S. Chang, S.-E. Park, G. Férey, A. K. Cheetham, *J. Am. Chem. Soc.* **2003**, *125*, 1309–1312.

[6] a) Ref. [1a]. For an earlier account, see: S. Kitagawa, M. Kondo, *Bull. Chem. Soc. Jpn.* **1998**, *71*, 1739–1753; b) G. Férey, *Chem. Mater.* **2001**, *13*, 3084–3098, and references therein.

[7] a) T. K. Maji, K. Uemura, H.-C. Chang, R. Matsuda, S. Kitagawa, *Angew. Chem.* **2004**, *116*, 3331–3334; *Angew. Chem. Int. Ed.* **2004**, *43*, 3269–3272; b) R. Wang, M. Hong, D. Yuan, Y. Sun, L. Xu, J. Luo, R. Cao, A. S. C. Chan, *Eur. J. Inorg. Chem.* **2004**, 37–43.

[8] a) R. Kitaura, F. Iwahori, R. Matsuda, S. Kitagawa, Y. Kubota, M. Takata, T. C. Kobayashi, *Inorg. Chem.* **2004**, *43*, 6522–6524; b) L. Pan, H. Liu, S. P. Kelly, X. Huang, D. H. Olson, J. Li, *Chem. Commun.* **2003**, 854–855.

[9] K. Kim and co-workers, unpublished results.

[10] M. E. Braun, C. D. Steffek, J. Kim, P. G. Rasmussen, O. M. Yaghi, *Chem. Commun.* **2001**, 2532–2533.

[11] The X-ray structure analysis from a single crystal as-synthesized is identical except for extensive disorder of guest molecules and is not reported here.

[12] The SQUEEZE routine of PLATON returns only five unaccounted electrons per unit cell.

[13] K. Seki, *Phys. Chem. Chem. Phys.* **2002**, *4*, 1968–1971.

[14] D. W. Breck, *Zeolite Molecular Sieves*, Wiley, New York, **1974**.

[15] X. Zhao, B. Xiao, A. J. Fletcher, K. M. Thomas, D. Bradshaw, M. J. Rosseinsky, *Science* **2004**, *306*, 1012–1015.

[16] The measured uptake in cm^3 g^{-1} was converted to weight percent by multiplying by a factor of 0.009.

[17] Assuming that monolayer condensation of hydrogen on a solid leads to a maximum 1.3×10^{-5} mol m^{-2}.[4b]

[18] T. Düren, L. Sarkisov, O. M. Yaghi, R. Q. Snurr, *Langmuir* **2004**, *20*, 2683–2689.

[19] a) A. Vishnyakov, P. I. Ravikovitch, A. V. Neimark, M. Bülow, Q. M. Wang, *Nano Lett.* **2003**, *3*, 713–718; b) A. I. Skoulidas, *J. Am. Chem. Soc.* **2004**, *126*, 1356–1357.

[20] A. L. Spek, PLATON, a multipurpose crystallographic tool, Utrecht University, Utrecht, The Netherlands, **2001**.

Received: November 24, 2004
Published online: March 11, 2005

